LIMNOLOGY
and
OCEANOGRAPHY

ASLO

Limnol. Oceanogr. 00, 2018, 00–00

doi: 10.1002/lno.10799

Effects of submarine groundwater discharge on coral accretion and bioerosion on two shallow reef flats

Katie A. Lubarsky [1], **Nyssa J. Silbiger** [2], **Megan J. Donahue** [1]*

[1]Hawai'i Institute of Marine Biology, University of Hawai'i at Mānoa, Kāne'ohe, Hawaii
[2]Department of Biology, California State University, Northridge, Northridge, California

Abstract

Submarine groundwater discharge (SGD) is an important source of nutrients to many coastal reefs, yet there is little information on how SGD impacts key coral reef processes. Here, we investigated the effect of SGD on coral growth and bioerosion rates from *Porites lobata* nubbins and blocks of calcium carbonate ($CaCO_3$) on two reef flats in Maunalua Bay, O'ahu. Over a 6-month (coral nubbins) and yearlong ($CaCO_3$ blocks) deployment period, we combined multiple metrics of coral growth (buoyant weight, surface area, and linear extension) and bioerosion with a suite of co-measured physicochemical parameters that are indicators for SGD (carbonate chemistry, dissolved inorganic nutrients, temperature, salinity, and water motion). All coral growth metrics showed a modal response to SGD, and the percent change in buoyant weights and nubbin surface area were negatively related to pH variation. SGD negatively affected coral survival, indicating that at high levels of SGD, salinity stress could be killing corals, but at mid-levels SGD-associated nutrients could be increasing growth rates. SGD had a positive effect on bioerosion, most likely due to the positive effect of increased nutrients on bioeroding organisms. Further, coral accretion rates were two orders of magnitude higher than bioerosion rates; however, given the low coral cover on these reef flats, the total carbonate accreted by corals is much lower than suggested by rates alone. These results indicate that corals can thrive on SGD-impacted reefs if isolated from secondary stressors, so active management to reduce macroalgae and sedimentation could allow coral recovery in Maunalua Bay.

Land-based inputs of freshwater are important sources of nutrients and other solutes to coastal reef ecosystems. Submarine groundwater discharge (SGD), defined as the flow of any water—meteoric, marine, or a composite of both—from land through the marginal seabed and into the coastal ocean (Moosdorf et al. 2015; Lee and Kim 2015), is an important source of terrigenous nutrients to many nearshore coral reefs. Globally, SGD makes up 6–10% of total freshwater inputs to the coastal ocean, with one-third of the global SGD component coming from large islands, particularly in the tropics (Moosdorf et al. 2015). On volcanic islands like Hawai'i, for example, SGD is abundant (Dimova et al. 2012; Richardson et al. 2017a), can exceed river fluxes, and often makes up the largest or only source of new nutrients to the coastal ocean (Johnson et al. 2008; Street et al. 2008; Moosdorf et al. 2015; Lee and Kim 2015). Unlike riverine inputs, which are driven by peaks in precipitation (Drupp et al. 2011), SGD is driven by hydrological gradients between the subterranean estuary and the coastal ocean and discharge is often tidally modulated, leading to diurnal or semidiurnal inputs on a daily basis (Dimova et al. 2012; Cyronak et al. 2013; Wang et al. 2014). The complex effects of SGD on coastal ecosystems, particularly coral reefs, remains understudied; however, the high volume and distinct water chemistry of SGD are likely to have strong impacts on key reef processes, such as accretion and bioerosion.

SGD is often highly enriched in nutrients, particularly nitrate, and can have N : P ratios that greatly exceed adjacent coastal water (Moosdorf et al. 2015). For example, in a study on the west coast of Hawai'i Island, average nutrient concentrations near groundwater seeps were generally 2–20 times higher than concentrations in offshore seawater (i.e., 14.9 μmol L^{-1} dissolved inorganic nitrogen (DIN) nearshore vs. 0.66 ± 0.24 μmol L^{-1} DIN offshore; Street et al. 2008). Groundwater has been identified as an important source of new nutrients to coastal systems (Paytan et al. 2006; Johnson et al. 2008; Street et al. 2008), especially in tropical systems where seawater can be highly oligotrophic (Moosdorf et al. 2015; Lee and Kim 2015). While high nutrient levels are a

*Correspondence: donahuem@hawaii.edu

Additional Supporting Information may be found in the online version of this article.

natural component of SGD, land-based pollution and other anthropogenic stressors can also elevate nutrient concentrations in SGD (Moosdorf et al. 2015; Richardson et al. 2017a). Because SGD is tidally driven, coastal systems subject to groundwater inputs often see pulses of nutrient-rich SGD on diurnal or semi-diurnal timescales, leading to elevated short-term variability.

In addition to high nutrient concentrations, SGD carries distinct carbonate signatures when compared with seawater and can drive changes in total alkalinity (TA), dissolved inorganic carbon, pH, and pCO_2 in nearshore environments (Cyronak et al. 2013, 2014; Wang et al. 2014). For example, in Rarotonga, Cyronak et al. (2014) found that freshwater SGD high in pCO_2 led to high pCO_2 in the surrounding seawater. Likewise, SGD in Rarotonga was also a source of TA to the fringing coral reef lagoon, with the highest fluxes at low tide (Cyronak et al. 2013).

In addition to directly driving variability in seawater chemistry due to mixing of SGD with seawater, SGD-derived solutes can affect biological processes, creating biogeochemical feedbacks that further modify the water chemistry of the coastal zone. For instance, Cyronak et al. (2014) found that pCO_2 variability off of Heron Island, Australia was augmented by stimulation of the photosynthesis/respiration cycle by SGD-derived nutrients. Despite the fact that SGD typically has lower pH than seawater, Lee and Kim (2015) found a negative relationship between salinity and pH across a groundwater gradient, indicating higher pH in areas with more SGD. They attributed this pattern to enhanced biological production driven by SGD nutrient inputs, rather than from the chemistry of the groundwater itself. However, in systems where SGD is particularly enriched in nutrients or where groundwater fluxes are especially high, groundwater chemistry can overwhelm biological processes and alter local seawater chemistry (Cyronak et al. 2014).

Although many coastal coral reefs, particularly those off of volcanic islands, are highly impacted by SGD, few studies exist on the effects of SGD on reef water chemistry, and even fewer investigate the effect of SGD on the metabolism of the organisms that inhabit reefs (but see, Richardson et al. 2017b; Prouty et al. 2018). For example, SGD is the major source of freshwater to the Kona coast of the Big Island of Hawai'i (Johnson et al. 2008; Street et al. 2008), an area which hosts some of the highest coral cover in the main Hawaiian Islands (Franklin et al. 2013). However, studies of SGD in this area are restricted to characterization of seawater chemistry across groundwater gradients, and effects on biology are only inferred. Likewise, in studies of SGD onto reefs in Rarotonga, Cook Islands and Heron Island, Australia, biological responses to SGD are inferred, but are not directly measured (Cyronak et al. 2013, 2014). Two exceptions are studies of calcification and bioerosion rates of corals near groundwater seeps in Maui and Mexico that found that calcification decreased and bioerosion increased near the seeps (Crook et al. 2013; Prouty et al. 2017).

Coral reefs persist in a balance between processes that build reefs, such as coral growth, and processes that break down carbonate structures, such as bioerosion and dissolution. Coral growth and bioerosion rates are both sensitive to changes in water chemistry, such as eutrophication (e.g., DeCarlo et al. 2015; Fabricius 2005) and seawater acidity (e.g., Andersson and Gledhill, 2013; Pandolfi et al. 2011; Silbiger et al. 2014; DeCarlo et al. 2015; Silbiger et al. 2016), which are altered by SGD. As SGD is a major contributor to seawater chemistry on high volcanic islands, it is important to understand how groundwater affects the accretion-erosion balance of nearshore reefs affected by SGD.

Maunalua Bay is an 8 km long embayment on the south shore of O'ahu, Hawai'i with several well-documented SGD-springs (Dimova et al. 2012; Swarzenski et al. 2013; Nelson et al. 2015; Richardson et al. 2017a). Land-use in Maunalua has shifted dramatically in the past century, from sparsely populated, rural developments in the early 1900s, toward rapid urbanization beginning in the 1960s (Wolanski et al. 2009). With increasing development, Maunalua Bay saw an increase in sedimentation and eutrophication due to dredging, stream channelization, and the use of on-site waste disposal systems, such as cesspools, resulting in decreased water quality and a decline in coral cover (Wolanski et al. 2009; Richardson et al. 2017a). However, the effect of SGD on the coral community in Maunalua Bay has never been formally quantified.

This study aims to understand the effects of SGD-driven chemical variability on the accretion-erosion dynamics of two nearshore reef flats in Maunalua Bay, O'ahu. We characterized short-term (diel- and tidal-scale) variability of a suite of chemical parameters across natural groundwater gradients at two SGD-impacted sites. We measured coral growth across the groundwater gradient by deploying nubbins of the lobe coral *Porites lobata* across each site for 6 months, comparing before and after buoyant weights and photographs and measuring the linear extension of each nubbin. In addition, we placed blocks of dead *Porites* skeleton, which act as a settling substrate for bioeroders, across the SGD gradient and measured rates of bioerosion after 1 yr by comparing pre- and post-deployment micro-computed tomography (μCT) scans. In this way, we were able to synthesize a comprehensive understanding of the effects of SGD on coral growth and bioerosion within these reefs.

Methods

Site selection

Two sites with previously identified SGD (Swarzenski et al. 2013; Nelson et al. 2015; Richardson et al. 2017a) were selected in Maunalua Bay. The sites, Black Point and Wailupe (Fig. 1), are shallow reef flats located 3 km apart, each with a discrete, nearshore SGD seep. Several diffuse

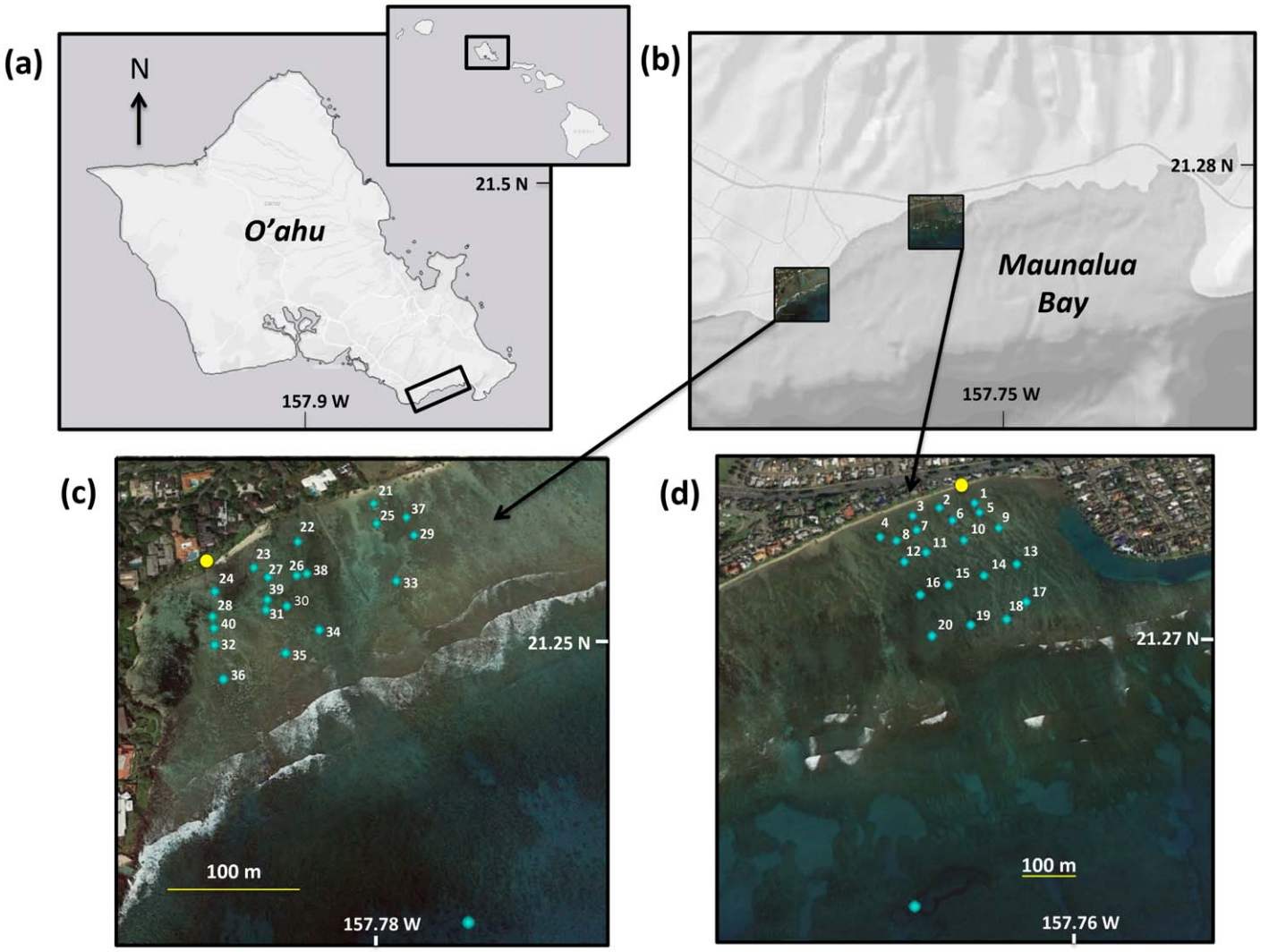

Fig. 1. (**a**) Map of the Hawaiian Islands and the island of O'ahu. Maunalaua Bay is enclosed in the black box. (**b**) Map of Maunalua Bay, with study sites enclosed in black boxes. Experimental locations, including offshore locations, are identified as blue dots at (**c**) Black Point and (**d**) Wailupe, and numbered with their unique waypoint number. The three offshore locations at each site are represented by a single point, as individual waypoints were not taken for these experimental units. Yellow dots represent the location of the groundwater seeps at each site and yellow lines are scale bars.

SGD seeps exist at both sites; however, the main seeps discharge a greater volume of water and were identified as the main groundwater source (Richardson et al. 2017a). The offshore bounds of each site were defined as the area from the shore to the reef crest (500 m at Wailupe, 250 m at Black Point), with the alongshore bounds chosen to capture the SGD gradient at each site (350 m at Wailupe, 250 m at Black Point). Both sites are very shallow (< 1 m deep at mean lower low water [MLLW]) and are characterized by patches of hard bottom surrounded by sand. The hard bottom at Wailupe is made up of carbonate platforms in a spur and groove pattern, whereas Black Point hosts a mix of continuous carbonate shelves and isolated boulders. Both sites are characterized by low coral cover and high macroalgal cover (Supporting Information Fig. 1). This is consistent with reports of decreased coral cover bay-wide, due to rapid urbanization and subsequent increases in sedimentation and decreases in water quality in the past few decades (Wolanski et al. 2009).

At each site, 20 experimental locations were established across the SGD gradient in an approximate grid (Fig. 1). All locations were established on hard carbonate substrate, except when carbonate substrate was absent and sites were established on basalt boulders (2 of 20 sites at Black Point). Three offshore locations were established outside of the reef crest at each site for a total of six offshore locations. Offshore locations were located in ~ 6–8 m of water, 200–350 m seaward of the reef crest and separated by at least 10 m.

Characterization of the SGD gradient

To characterize water chemistry across the SGD gradient, water was collected at each experimental location at high and low tides (day and night, or four samples per 24 h) over two 24-h cycles (totaling eight samples per location) and analyzed for a suite of chemical parameters. Sampling dates were chosen to coincide with maximum spring tides during the spring and the fall of 2015, in order to capture the strongest groundwater gradient, highest possible chemical variability, and to account for seasonality. Sampling dates were 18 April 2015 and 28 September 2015 at Wailupe and 02 May 2015 and 26 October 2015 at Black Point.

Samples for pH, TA, and inorganic nutrients (SiO_4^{2-}, $NO_3^- + NO_2^-$, and PO_4^{3-}) were hand-collected from each experimental location within ± 30 min of low and high tides during both the day and night for each sampling period (spring and fall): a total of eight samples at each location. Water samples were collected at each experimental unit by submerging a capped sample bottle, opening and filling it directly above the experimental unit, and recapping it underwater, in order to capture the chemistry of the water directly impacting the experimental corals and blocks. Samples were collected into acid-washed and triple-rinsed polypropylene sample bottles and then filled completely so that no head space remained. Samples were immediately processed or appropriately stored following standard protocols described below.

pH and TA

pH on the total scale (pH_{Tot}) was measured using an Orion ROSS Ultra pH/ATC Triode calibrated against a Tris buffer of known pH from the Dickson laboratory at the Scripps Institution of Oceanography (Dickson et al. 2007). Calculated pH values were corrected based on in situ temperature recorded by the temperature loggers at each experimental location using CO_2SYS (Lewis and Wallace 1998).

TA samples were fixed immediately following collection with 100 μL $HgCl_2$ per 250 mL water and technical duplicates (mean SE = 2.68 μEq) were analyzed using open cell potentiometric titrations on a Mettler Toledo T-50 autotitrator. Acid concentrations were calibrated against certified reference materials (CRM) from Andrew Dickson's lab following Dickson et al. (2007) protocols. All samples were measured within 1% accuracy of the CRM value (mean deviation from CRM value = 0.48% ± 0.33% SD) and measured values were corrected based on the deviation from the CRM value.

Inorganic nutrients

Nutrient samples were filtered through combusted 25 mm glass fiber filters (GF/F 0.7 μm) immediately after collection. Filtered samples were stored in acid-washed polypropylene bottles and refrigerated until analysis. Nutrient analysis for SiO_4^{2-}, $NO_3^- + NO_2^-$, and PO_4^{3-} was performed in the SOEST Laboratory for Analytical Biogeochemistry (S-LAB) at the University of Hawai'i at Mānoa using a Seal Analytical AA3 Nutrient Autoanalyzer. Reported error (coefficient of variation) for nutrient analyses are 0.5% for SiO_4^{2-}, 0.3% for $NO_3^- + NO_2^-$, and 0.2% for PO_4^{3-}.

Salinity

Salinity values were calculated using known relationships between silicate and salinity at each site reported by Richardson et al. (2017a). Silicate has been used successfully as an SGD tracer in Hawai'i (Street et al. 2008), and silicate uptake is at most 10% of the total inventory at these sites (Richardson et al. 2017a). Silicate and salinity were found to mix conservatively at levels of silicate below ~ 300 ML^{-1} ($R^2 = 0.99$ at each site; residual mean square error = 0.191 at Wailupe, 0.170 at Black Point), and the highest recorded silicate value in our study was 198.43 μML^{-1}. Because salinity values were not directly measured in the field, silicate was used as the SGD tracer in this study, and salinity values estimated from the silicate-salinity relationship at each site were used to calculate carbonate parameters.

Relative water motion

Relative water motion was measured using the clod card method (Doty 1971). Clod cards were made from plaster of Paris using ratios of water and plaster adapted from Jokiel and Morrissey (1993). The plaster was poured into ice cube trays, tapped to remove bubbles, and dried in a drying oven at 60°C for 24 h. Dry clods were sanded to a standard mass of 25 g (± 0.1 g), glued to small squares of flexible plastic, and reweighed to determine total pre-deployment weights.

Three replicate clod cards were deployed at each experimental location for 4 h bracketing a spring low and high tide at each location (Black Point on 01 August 2015 and at Wailupe on 12 September 2015). After recovery, clod cards were dried in a drying oven at 60°C for 24 h and reweighed to calculate change in mass during the deployment. Field measurements were normalized for the rate of clod dissolution in standing water by placing six control clod cards in separate stagnant aquaria for 4 h to match the length of deployment in the field. In order to account for differences in clod dissolution due to salinity (Jokiel and Morrissey 1993), control aquaria were separated into three high and three low salinity treatments of 35 and 27, respectively, in order to cover the range of salinities recorded across the SGD gradients at both sites. Experimental locations were separated into high and low salinity categories based on measured salinity values at low and high tide, and values from the corresponding control treatment were used in calculations. The dissolution factor (DF), a dimensionless index of clod dissolution, for each clod card was calculated using the equation in Doty (1971). High and low tide values were averaged to calculate the mean DF for each experimental location.

Temperature

Temperature was recorded every 15 min at all experimental locations throughout the deployment period by HOBO

Table 1. Summary statistics of chemical and physical drivers. Measurements for silicate, nitrate + nitrite (N + N), phosphate, pH, TA, and temperature are from discrete water samples in the spring and fall.

Site	Parameter	Mean	Maximum	Minimum	Standard deviation
Wailupe	Silicate (μmol L^{-1})	15.60	198.43	1.03	33.74
	Salinity (psu)	33.99	34.64	25.96	1.48
	N + N (μmol L^{-1})	0.73	11.69	0.04	1.69
	Phosphate (μmol L^{-1})	0.13	0.62	0.040	0.10
	pH_{Tot}	8.02	8.20	7.85	0.084
	TA (μEq L^{-1})	2252.11	2336.32	2129.37	34.34
	Temperature (°C)	25.30	28.50	22.64	1.29
	Clod DF	4.43	6.26	3.14	0.93
	Depth (m at MLLW)	0.32	0.81	0.0030	0.23
Black Point	Silicate (μmol L^{-1})	16.27	136.95	1.09	22.70
	Salinity (psu)	34.04	34.67	29.00	0.95
	N + N (μmol L^{-1})	2.79	32.39	0.020	4.95
	Phosphate (μmol L^{-1})	0.20	0.89	0.090	0.13
	pH_{Tot}	8.06	8.33	7.86	0.11
	TA (μEq L^{-1})	2271.54	2413.56	2005.77	45.04
	Temperature (°C)	25.75	28.80	23.45	1.36
	Clod DF	4.39	5.99	3.44	0.63
	Depth (m at MLLW)	0.58	0.86	0.31	0.16

TidbiT v2 loggers (accuracy: ± 0.2°C, resolution: 0.02°C at 25°C) attached to each bioerosion block. Each logger was coated in Plasti-Dip Multipurpose Rubber Coating to prevent damage and cable tied to the Polyvinyl chloride (PVC) mount on each bioerosion block. Following deployment, loggers were placed in water in a single aquarium and calibrated to a reference thermometer, and time series were adjusted for this calibration.

Time series were truncated to correspond with the dates of deployment for coral nubbins and bioerosion blocks. Due to a loss of loggers at the beginning of the deployment, time series for the bioerosion blocks only cover the period of February–November 2015. The difference in mean temperature between the collection site and the experimental location (Δ mean T) was calculated as

$$\Delta \text{mean } T = \text{mean } T_{\text{experiment}} - \text{mean } T_{\text{collection}}$$

with mean $T_{\text{experiment}}$ referring to the mean temperature at each experimental unit, and mean $T_{\text{collection}}$ referring to the mean temperature at the offshore location where the coral fragments were collected. This deviation is positive if nubbins experienced hotter than average temperatures, and negative if temperatures were below average.

Depth

Depth at each experimental location was measured from the surface using a weighted transect tape, and the time of each depth measurement was recorded. Measurements were normalized to tidal height at MLLW. Tide predictions were obtained from the Honolulu tide gauge station (NOAA Station ID 1612340), and offsets in the timing of tidal predictions were calculated using data from a stationary depth sensor placed nearshore at Black Point for 4 d in August 2015.

Coral growth

In order to assess the effect of SGD on coral growth rates, *P. lobata* nubbins were deployed at each of the experimental locations at both sites for a period of 6 months, from February 2015 to August 2015 (Supporting Information Table 1). *P. lobata* was chosen because it is present at both sites and is abundant in Maunalua Bay. Fragments were collected from three large colonies near the offshore experimental locations at Wailupe at a depth of approximately 8 m. Offshore donor colonies were chosen to avoid any acclimation of corals to SGD. Nubbins were attached to PVC plates, which acted as the experimental units in the study. Nubbins were prepared and analyzed before and after deployment, respectively, at the Anuenue Fisheries Research Center in Honolulu, Hawai'i.

To establish the experiment, fragments collected from each donor colony were kept separate and immediately placed in a 10 mg L^{-1} Alizarin red solution for 24 h, and then placed in flow-through water tables. Small nubbins (area of live tissue ~ 2 cm^2) were cut from the fragments using tin snips (Forsman et al. 2006) and three nubbins from the same donor colony were mounted on PVC plates using All-Fix epoxy.

Each plate was buoyant weighed in seawater using an Ohaus Adventurer Pro precision balance before and after deployment in the field following Jokiel et al. (1978). The buoyant weight of the PVC plate itself was subtracted from the total weight in order to calculate the weight of the

nubbins, and plates were thoroughly cleaned of all sediment, algae and other organisms before post-deployment weighing. Coral growth was reported as percent change in buoyant weight. Because buoyant weight measurements were taken at the plate scale, only plates with all nubbins attached were included in the analysis.

In addition, standardized photos of each plate were taken before and after deployment using a camera mounted on a PVC camera stand. Each plate was photographed from above with a size standard in each photo. Total surface area of each nubbin (including areas of partial or full mortality where tissue had grown and died away) was calculated in Adobe Photoshop by calibrating the measurement tool to the size standard and hand-outlining live tissue on each coral nubbin. Coral growth was reported as the percent change in surface area. Survivorship was determined using the post-deployment standardized photos. In order to understand which locations were optimal for coral survival vs. those leading to a degraded or completely dead state, coral survivorship was recorded as a percentage of live tissue.

At each experimental location, three coral plates, each with three nubbins from a single donor colony, were attached to upward-facing bolts, for a total of nine nubbins (three per donor colony) at each location. Sustained high water temperatures during late summer 2015 forced the removal of coral plates after 174 d in order to avoid bleaching-related mortality.

After the post-deployment buoyant weights and photos were collected, nubbins were removed from the plates and a slice was extracted from the middle of each nubbin, perpendicular to the axis of extension, using a diamond blade saw (Supporting Information Fig. 2). Coral slices were photographed under a dissecting scope for linear extension analysis. In Adobe Photoshop, the perpendicular distance from the Alizarin red band to the edge of the coral was recorded from three evenly spaced locations chosen a priori in order to compute a mean value that captures variation in growth across the coral nubbin. Extension measurements were calibrated to a size standard photographed under the same magnification. Linear extension is reported in mm rather than as a rate (mm yr^{-1}) as coral nubbins were only deployed for 6 months, so these data do not account for seasonality in growth.

Bioerosion

Experimental blocks were cut from dead *P. lobata* rubble collected from above the high tide mark. Coral skeletons were cut into blocks measuring 6 cm × 5 cm × 1.5 cm using a diamond blade rock saw and were attached to a PVC mount at one end using JB Weld Steel Reinforced two part epoxy. Only blocks without visible calices or boreholes were used.

Blocks were scanned before and after deployment using μCT at the Multiscale CT Facility at Cornell University using an eXplore CT120 μCT (GE Healthcare Xradia) in order to construct a three-dimensional image of object densities in the interior and exterior of each block (Silbiger et al. 2014; Silbiger et al. 2016; Silbiger et al. 2017). μCT analysis followed methods outlined in Silbiger et al. (2016). Pre- and post-deployment scans were registered using an intensity-based image registration algorithm from the MATLAB Image Processing Toolbox, each pixel converted to binary (1 = a pixel with $CaCO_3$, 0 = Air), and scans were subtracted from each other in order to identify areas of bioerosion. Pixels with a subtracted value of −1 represented areas of bioerosion, and pixels with subtracted values of 0 represented areas of no change. Pixels with a subtracted value of +1 represented areas of $CaCO_3$ accretion to the block; however, high amounts of sedimentation on the blocks lead to an overestimation of accretion, so accretion rates were excluded from the analysis.

Bioerosion volume was calculated by summing all negative subtracted values, and multiplying by the voxel size $(100\ \mu m)^3$ to give the total volume of the $CaCO_3$ lost. Bioerosion rates were calculated using the following equation

$$\text{Bioerosion rate}\left(\text{kg m}^{-2}\ \text{yr}^{-1}\right) = \frac{\text{Vol}_i \times \rho_i}{\text{SA}_i \times \text{Time}}$$

where i represents each block, Vol is the volume of $CaCO_3$ lost through bioerosion in m^3, ρ is the skeletal density of the blocks in g cm^{-3} (average skeletal density of the blocks was 1.42 ± 0.07 [SD] g cm^{-3}), SA is the surface area of the block in m^2, and Time is the time the block was deployed on the reef in years. Surface area of each block was measured by hand using calipers and excluded the surface of the block adhered to the PVC mount, as this surface was not available to bioeroders.

One bioerosion block was deployed at each of the 46 experimental locations described above (40 on the reef flats, and 6 at the offshore locations). Blocks were threaded onto upward-facing bolts through a hole in the PVC mount and secured with two stainless steel nuts. An Onset HOBO TidbiT v2 temperature logger was attached to each block and set to record temperature every 15 min. Blocks were deployed between 29 October 2014 and 14 November 2014, with lost blocks replaced with new ones until December 2014 ($n = 1$ at Wailupe, $n = 3$ at Black Point), and recovered between 16 November 2015 and 18 November 2015 on the reef flats, and on 04 December 2015 at offshore sites (Supporting Information Table 1). After recovery, blocks were dried in a drying oven at 60°C for 24 h and sent to the Cornell University Biotechnology Resource Center for post-deployment μCT scanning.

Statistical analysis

Due to the approximately conservative mixing of SGD-derived solutes with seawater at these sites, nutrients ($NO_3^- + NO_2^-$, PO_4^{3-}) and TA were highly correlated with

silicate at each site ($0.97 < |\rho| < 0.98$ for phosphate, $0.97 < |\rho| < 0.99$ for N + N, and $0.68 < |\rho| < 0.82$ for TA; Supporting Information Figs. 3, 4). This high collinearity prevented the separate analysis of individual SGD-derived solutes and only silicate was included as a groundwater tracer in the models; nutrients and TA were assumed to covary with SGD in all analyses. Because the groundwater endmembers at each site contain different ratios of silicate to nutrients (Richardson et al. 2017a), a standardized measurement of groundwater was calculated as

$$\%\,\mathrm{SGD} = \frac{\mathrm{Silicate_{mix}} - \mathrm{Silicate_{SW}}}{\mathrm{Silicate_{GW}} - \mathrm{Silicate_{SW}}}$$

where $\mathrm{Silicate_{mix}}$ is the mean value at each experimental location, $\mathrm{Silicate_{GW}}$ is the value of the groundwater endmember at each site (Black Point = 800 μM or Wailupe = 781 μM; values from Richardson et al. 2017a), and $\mathrm{Silicate_{SW}}$ is the value of the seawater endmember (1.03 μM), as identified as the lowest silicate value recorded in this experiment. pH was not correlated with groundwater (Supporting Information Figs. 3, 4), so mean pH and pH variation at each experimental location were included in the models. pH variation was calculated as

$$\mathrm{pH\ variation} = \frac{\mathrm{Variance_{pH}}}{\mathrm{Mean_{pH}}^2}$$

in order to obtain a measure of dispersion independent of the mean. Relative water motion was included in the models as mean DF at each experimental location.

The estimated mean coral accretion rates at each experimental location were calculated using the following formula:

$$\mathrm{Coral\ accretion\ rate}\left(\mathrm{kg\ m^{-2}\ yr^{-1}}\right) = \frac{\Delta \mathrm{BW_{plate}}}{\mathrm{SAinit_{plate}} \times \mathrm{time}}$$

where $\Delta \mathrm{BW_{plate}}$ is the change in buoyant weight for a single coral plate in kg, $\mathrm{SAinit_{plate}}$ is the initial surface area of all three nubbins on the plate in $\mathrm{m^2}$, and time is the time of deployment in years.

Offshore sites were not included in the analyses due to weather and gear restrictions, which prevented the collection of water samples at these locations. However, response values for coral growth and bioerosion from offshore locations are included in Fig. 4 to indicate how offshore units compared to inshore units.

In order to account for the hierarchical structure of the coral experiment and the use of nubbins from three different donor colonies, percent change in buoyant weight, percent change in surface area, and linear extension were analyzed using linear mixed effects models, and survivorship was analyzed using a mixed effects logistic regression. Because the bioerosion experiment was not hierarchically structured (only one bioerosion block per location), these data were analyzed using a simple linear regression. In order to account for apparent nonlinearity in the data, $\%\mathrm{SGD}^2$ was included in all coral growth models, while $\sqrt{}\%\mathrm{SGD}$ was included in the bioerosion model. The model equations for percent change in buoyant weight (%ΔBW; Eq. 1), percent change in surface area (%ΔSA; Eq. 2), linear extension (LE; Eq. 3), survivorship (Eq. 4) and bioerosion rate (Eq. 5) are shown below.

$$\%\Delta\mathrm{BW} \sim \%\mathrm{SGD} + \%\mathrm{SGD}^2 + \mathrm{pH} + \mathrm{pH\ Variation} + \Delta\,\mathrm{mean}\ T + \mathrm{DF} + (1|\mathrm{Location}) + (1|\mathrm{Donor\ Colony}) \quad (1)$$

$$\%\Delta\mathrm{SA} \sim \%\mathrm{SGD} + \%\mathrm{SGD}^2 + \mathrm{pH} + \mathrm{pH\ Variation} + \Delta\,\mathrm{mean}\ T + \mathrm{DF} + (1|\mathrm{Plate/Location}) + (1|\mathrm{Donor\ Colony}) \quad (2)$$

$$\mathrm{LE} \sim \%\mathrm{SGD} + \%\mathrm{SGD}^2 + \mathrm{pH} + \mathrm{pH\ Variation} + \Delta\,\mathrm{mean}\ T + \mathrm{DF} + (1|\mathrm{Plate/Location}) + (1|\mathrm{Donor\ Colony}) \quad (3)$$

$$\mathrm{Survival} \sim \%\mathrm{SGD} + \mathrm{pH} + \mathrm{pH\ Variation} + \Delta\,\mathrm{mean}\ T + \mathrm{DF} + (1|\mathrm{Plate/Location}) + (1|\mathrm{Donor\ Colony}),\ \mathrm{family} = \mathrm{binomial} \quad (4)$$

$$\mathrm{Bioerosion\ rate} \sim \sqrt{\%\mathrm{SGD}} + \mathrm{pH} + \mathrm{pH\ Variation} + \Delta\,\mathrm{mean}\ T + \mathrm{DF} \quad (5)$$

Results

Site characterization

Wailupe saw a wider range of %SGD values with mean %SGD ranging from 0.06% to 8.67%, whereas mean values at Black Point ranged from 0.09% to 4.35%. However, because of higher levels of nutrients in the groundwater endmember at Black Point (Richardson et al. 2017a), the range of nutrients delivered to the experimental units was similar at both sites (Table 1, Supporting Information Fig. 5). Interestingly, although TA correlated highly with SGD, the TA gradient was opposite between the sites, with TA in SGD at Black Point higher than the marine endmember, and lower than the marine endmember at Wailupe (Supporting Information Fig. 6). This is consistent with previous studies (Nelson et al. 2015; Richardson et al. 2017b) and is likely due to the fact that SGD at each site is derived from separate aquifers (Richardson et al. 2017a,b). TA values converge at the lowest values of %SGD, indicating that we captured the marine endmember at both sites. pH varied between 7.86 and 8.33 at Black Point and 7.85 and 8.20 at Wailupe, while mean pH was similar between sites (BP = 8.06, W = 8.02; Table 1).

DF was similar across sites, with a slightly wider range and higher mean at Wailupe, likely due to the greater size of the site allowing for more heterogeneity in water motion. All experimental locations were less than 0.9 m deep at MLLW, with Black Point slightly deeper on average. The shallowest location at Wailupe was 0.003 m at MLLW and was likely exposed during spring low tides.

Table 2. Summary statistics of response variables. Negative values likely reflect physical damage to nubbins during the deployment.

Site	Response variable	Mean	Maximum	Minimum	Standard deviation
Wailupe	Percent change in buoyant weight (%)	39.87	114.41	5.85	21.95
	Percent change in surface area (%)	79.81	242.23	−51.94	52.23
	Linear extension (mm 6 mo^{-1})	1.87	4.34	0.32	0.88
	Coral accretion rate (kg m^{-2} of live coral yr^{-1})	10.34	16.52	2.91	3.83
	Bioerosion rate (kg m^{-2} yr^{-1})	0.047	0.19	0.0034	0.042
Black Point	Percent change in buoyant weight (%)	43.26	88.64	−9.17	20.82
	Percent change in surface area (%)	102.19	627.76	−74.66	79.84
	Linear extension (mm 6 mo^{-1})	1.81	6.18	0.33	1.01
	Coral accretion rate (kg m^{-2} of live coral yr^{-1})	11.86	19.48	5.83	4.16
	Bioerosion rate (kg m^{-2} yr^{-1})	0.042	0.082	0.0093	0.025

Coral accretion, survivorship, and bioerosion

Coral accretion rates (derived from buoyant weight and surface area of the corals) were two orders of magnitude higher than bioerosion rates and ranged between 2.91 kg m^{-2} and 19.48 kg m^{-2} of live coral yr^{-1}, with a mean of 11.06 ± 4.01 (SD) kg m^{-2} of live coral yr^{-1} (Table 2). Bioerosion rates ranged between 0.003 kg m^{-2} yr^{-1} and 0.174 kg m^{-2} yr^{-1} with a mean of 0.040 ± 0.032 (SD) kg m^{-2} yr^{-1}. Percent changes in buoyant weights of plates were substantial, with maximum values exceeding 100%, while percent changes in surface areas of individual nubbins exceeded 600%. Both percent change in buoyant weight and surface area had minimum values less than 0%, indicating negative growth; this is likely due to physical damage that removed carbonate during the deployment. The fastest linear extension rates were comparable to those found for *P. lobata* in Hawai'i (Grottoli 1999) and Indonesia (Edinger et al. 2000), with maximum linear extension at 6.18 mm over the 6-month deployment, compared with a minimum of 0.32 mm and a mean of 1.85 mm ± 0.94 (SD).

Buoyant weight and surface area showed a significant negative effect of $\%SGD^2$, indicating a modal response of coral growth to %SGD (Table 3). $\%SGD^2$ was nearly significant in the linear extension model, as well ($p = 0.058$). In addition, %SGD showed a significant positive effect on percent change in surface area and buoyant weight. pH variation had a significant negative effect on percent change in buoyant weight and percent change in surface area. Increasing %SGD decreased survivorship (Supporting Information Fig. 7); no other fixed effects were significant for survivorship. Spatial patterns of all coral growth metrics and significant drivers can be found in Figs. 2, 3.

Patterns in the random effects were not consistent between models. Donor colony accounted for 33.70% of the variance in the buoyant weight model, but only 1.25% in the surface area model. Colony accounted for 0% of the variance in the linear extension model, so it was dropped from this model. Model coefficients from the buoyant weight and surface area models indicate that colony B had the highest growth rates (Table 3). However, in the survivorship model, where donor colony accounted for 29.16% of the variance, colony A had the highest rate of survivorship. Plate and experimental location accounted for 7.85% and 2.69% of the variance in the surface area model, 4.09% and 8.89% in the linear extension model, and 47.36% and 23.47% in the survivorship model, respectively. Experimental location accounted for 0% of the variance in the buoyant weight model and was dropped from the final analysis.

$\sqrt{\%SGD}$ had a significant positive effect on bioerosion, indicating that bioerosion increases nonlinearly with %SGD. None of the other terms in the model showed a significant response. The overall model was significant and explained 35.77% of the variance ($p = 0.02$, $R^2 = 0.36$).

Discussion

SGD effects on coral growth and survivorship

All three coral growth metrics showed a modal response to SGD, with the highest growth rates at mid-range SGD values. The low coral growth rates and survivorship in the presence of high SGD are likely due to salinity stress, whereas higher growth rates at moderate levels of SGD are likely due to moderate increases in nutrients. The strength of this relationship relative to other terms, and the fact that this was the only consistent pattern across all three growth metrics, suggests that SGD is the main driver of differences in coral growth across these reef flats. This is consistent with results from Richardson et al. (2017b), which found that SGD drives patterns in net community calcification across these sites. Because of the near-conservative nature of SGD-derived solutes at the sites (Richardson et al. 2017a), water chemistry (silicate, nutrients, TA) at each experimental location was likely driven by physical mixing of the groundwater with seawater, rather than by reef metabolism.

At the highest levels of SGD, coral growth and survivorship were lowest. High levels (> 5%) of SGD were only

Table 3. Summary of significant model results and random effects. Empty cells signify nonsignificant terms; NA indicates that a term was not included in the final model. Random effects that accounted for 0% of the variance were excluded from the final model. An asterisk indicates that the term is not significant, but is displayed to demonstrate patterns in the data. Values for fixed effects indicate the coefficient of each term (β), t values, and p values. Values for random effects are the percentage of variance explained by each term; for colony, the coefficients for colonies A, B, and C are listed below this value.

	Fixed effects							Random effects		
Response	%SGD	%SGD^2	$\sqrt{}$%SGD	pH	pH variation	Δ mean T	DF	Plate	Experimental location	Colony
Percent change in buoyant weight	β=0.57, t=2.008, p=0.049	β=−0.55, t=−3.624, p<0.001	NA	—	β=−0.42, t=−2.290, p=0.025	—	—	NA	NA	33.7% A: −0.62 B: 0.87 C: −0.26
Percent change in surface area	β=55.01, t=5.611, p<0.001	β=−32.66, t=−6.472 p<0.001	NA	—	β=−20.52, t=−3.236, p=0.003	—	—	7.85%	2.69%	1.25% A: −4.67 B: 4.70 C: −0.03
Linear extension	—	β=−0.18, t=−1.981, p=0.058*	NA	—	—	—	—	4.09%	8.89%	NA
Survivorship	β=−1.05, p<0.001	NA	NA	—	—	—	—	47.36%	23.47%	29.16% A: 0.47 B: 0.01 C: −0.91
Bioerosion	NA	NA	β=0.01 p=0.02	—	—	—	—	NA	NA	NA

observed at Wailupe as low water motion and shallow depth nearshore allowed for less mixing and higher delivery of SGD to nearshore experimental locations (Fig. 2b), leading to high mortality and little coral growth close to shore; although the same pattern of survivorship exists at Black Point at similar levels of SGD. Indeed, SGD was the only significant predictor of survivorship and the best predictor of coral growth across sites. Initial surface area of nubbins had no significant effect on survivorship, which is consistent with previous studies on the survivorship of small *P. lobata* nubbins (Forsman et al. 2006), and indicates that differences were due to environmental factors.

The decrease in survivorship and coral growth at high SGD is likely due to salinity stress, with calculated mean salinity values of 31.6 at the highest SGD sites and low tide minimum values as low as 25.9. This is consistent with a recent study from Maui, Hawai'i where *P. lobata* colonies exposed to salinities < 33 near an SGD seep were dead, but colonies further from the seep exposed to higher salinity (33–36) were alive (Prouty et al. 2017). Similarly, data from Richardson et al. (2017b) indicate that low salinity near SGD seeps at these sites stresses calcifying organisms and leads to low calcification rates.

Elevated nutrients are generally found to be detrimental to coral health and calcification (reviewed in Fabricius 2005), and nutrients from SGD have been implicated in reef degradation (Nairn 1993). However, some studies have found either no effect of nutrients on coral growth (Edinger et al. 2000), or have seen moderate (Tanaka et al. 2007; Sawall et al. 2011) or large increases in coral growth in response to elevated nutrients (Bongiorni et al. 2003). Indeed, Chauvin et al. (2011) found that corals collected from areas affected by high-nutrient SGD had higher chlorophyll *a*, protein and *Symbiodinium* densities, and showed higher rates of photosynthesis and calcification per unit surface area than corals collected from SGD-free locations. Importantly, studies that have found increased growth rates under elevated nutrient conditions isolated corals from secondary effects of nutrient enrichment, such as competition with macroalgae (Bongiorni et al. 2003). Similarly, coral plates in this study were elevated above the substrate; therefore, the corals were released from competition with benthic macroalgae and from some of the sedimentation stress, allowing the effect of nutrients on coral growth to be isolated from confounding processes.

Because of the conservative nature of groundwater mixing at these sites, it was impossible to disentangle SGD-derived solutes (nutrients, TA) from silicate, making it difficult to quantitatively determine the relative importance of each parameter in driving the observed coral growth patterns. However, examination of the TA data from both sites reveals opposite effects of SGD on alkalinity concentrations (Supporting Information Fig. 6), with groundwater at Black Point

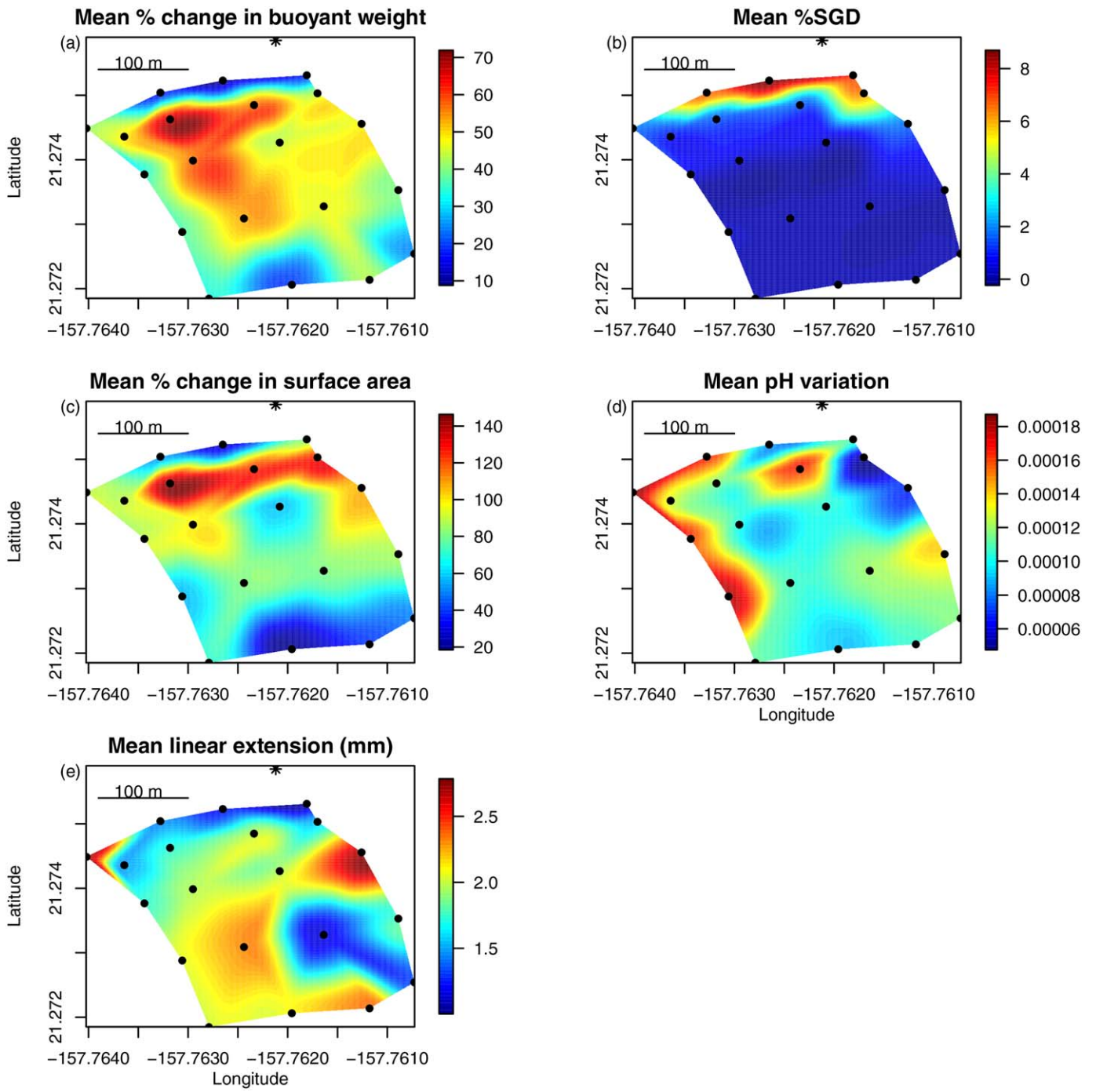

Fig. 2. Contour plots of response variables (**a**, **c**, **e**) and significant drivers (**b**, **d**) of coral growth at Wailupe. Black dots indicate experimental locations, and the star indicates the location of the groundwater seep.

having higher and Wailupe having lower TA values than the surrounding seawater, and converging to the same marine endmember value. This pattern is consistent with findings by Nelson et al. (2015), and is likely due to the fact that SGD at these sites is derived from two isolated aquifers, each with a distinct water chemistry (Richardson et al. 2017a,b). Although it has been hypothesized that inputs of TA from SGD may affect reef health by buffering against the negative effects of ocean acidification (Cyronak et al. 2013, 2014), it is unlikely that TA affected coral growth in this case as growth patterns were similar across sites, despite opposite patterns in TA.

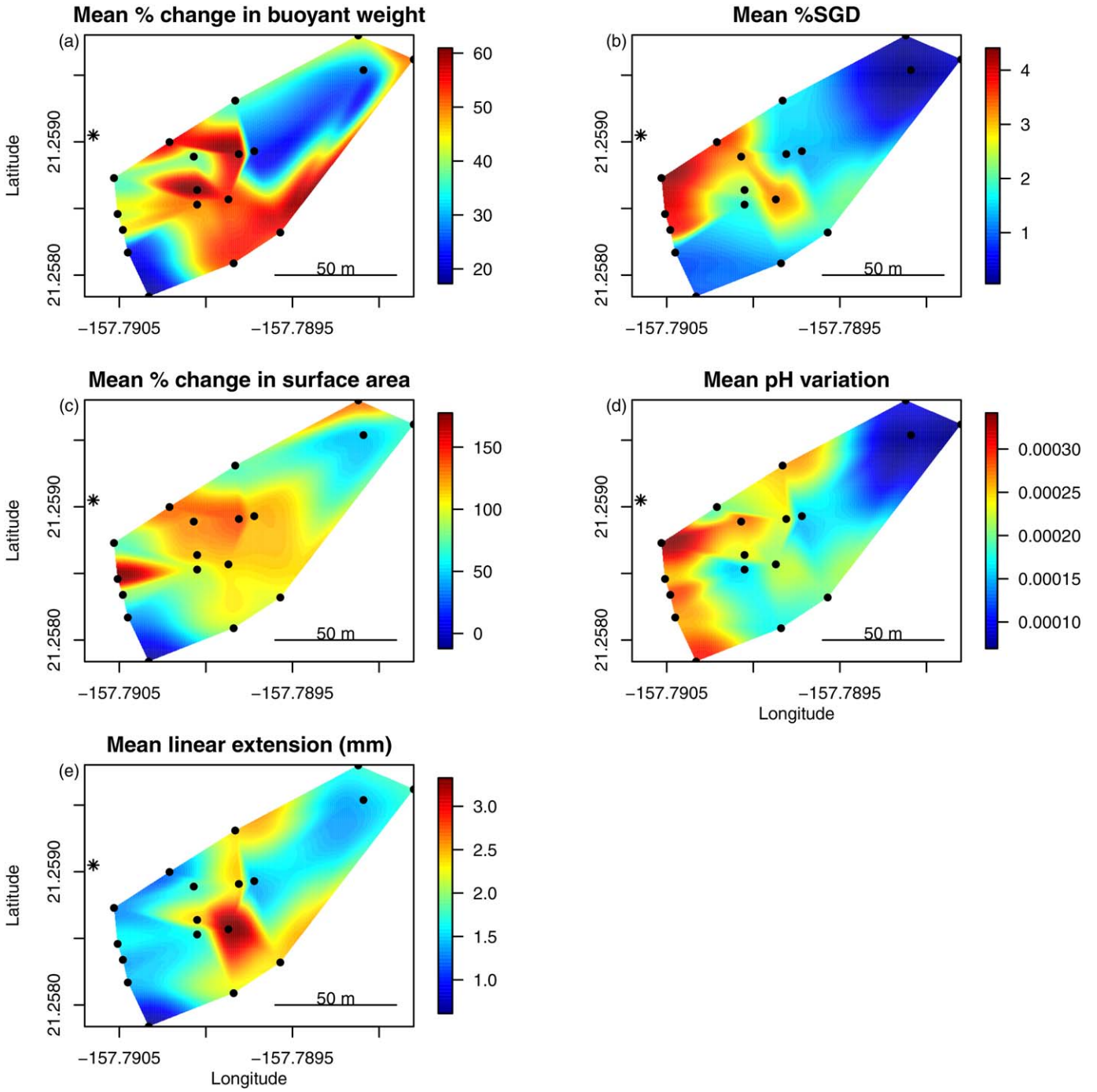

Fig. 3. Contour plots of response variables (**a**, **c**, **e**) and significant drivers (**b**, **d**) of coral growth at Black Point. Black dots indicate experimental locations, and the star indicates the location of the groundwater seep. Note that experiments from two locations were lost, resulting in only 18 data points for this site.

SGD effects on bioerosion

Bioerosion also showed a positive nonlinear response to SGD. However, unlike coral growth, bioerosion rates did not decrease at high levels of SGD, and instead leveled off at a maximum around 3% SGD. This indicates that bioerosion is less sensitive to low salinities than coral growth, and that SGD-derived nutrients likely increase bioerosion rates until nutrients become saturating or conditions become stressful, at which point bioerosion rates plateau. This is consistent with previous studies that have noted increased bioerosion with increasing nutrients (Edinger et al. 2000; Holmes 2000; Le Grand and Fabricius 2011). Studies that have assessed

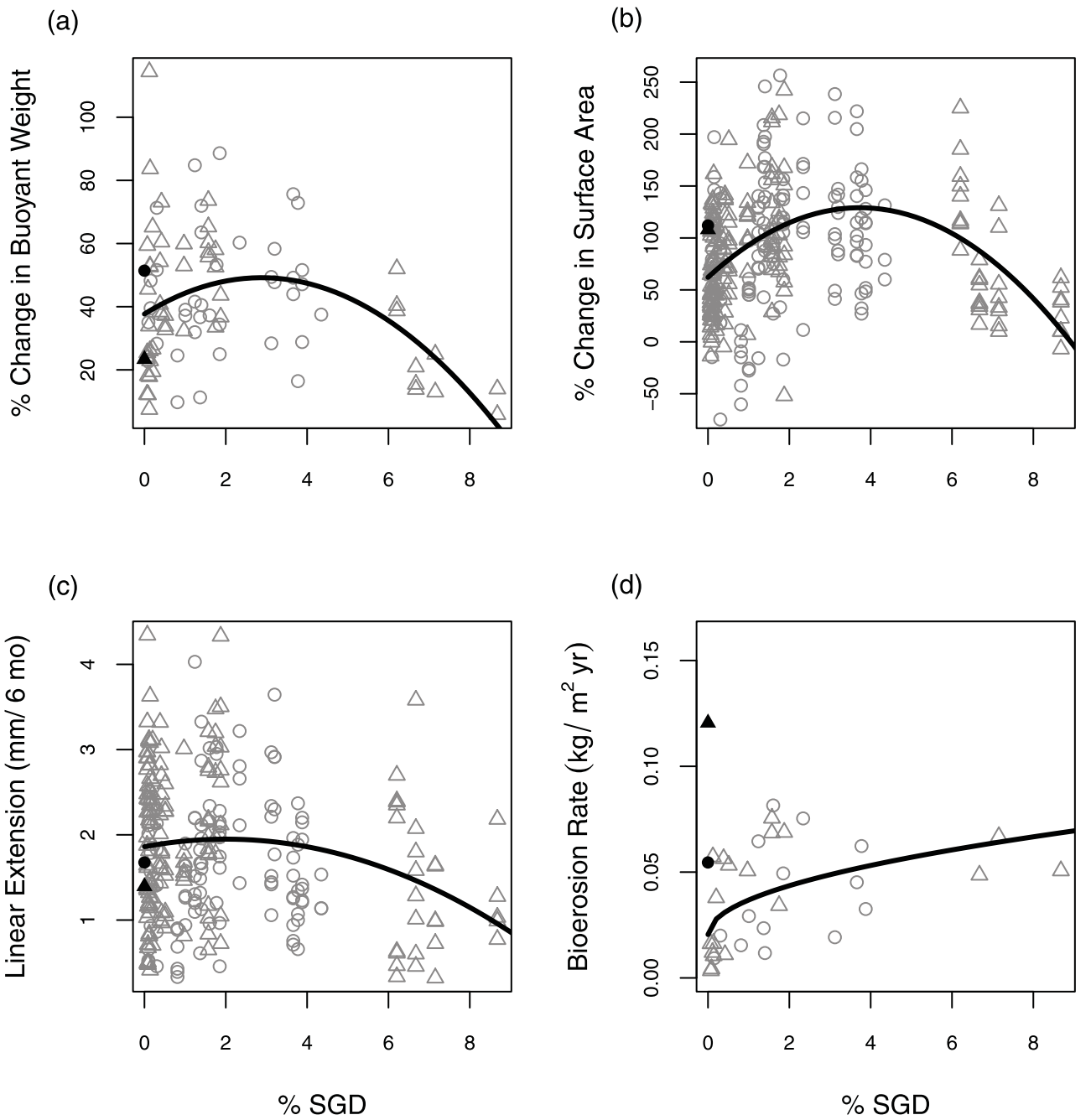

Fig. 4. Plots of %SGD vs. (**a**) percent change in buoyant weight, (**b**) percent change in surface area, (**c**) linear extension, and (**d**) bioerosion rate. Open triangles indicate data from Wailupe; open circles indicate data from Black Point. The black triangle and circle are the mean values of each response at the offshore Wailupe and Black Point sites, respectively, and have been plotted at 0% SGD in lieu of chemical data. The black line represents the best fit between the data and %SGD: (**a**) $y = -1.39x^2 + 8.00x + 37.69$, (**b**) $y = -4.80x^2 + 35.89x + 62.11$, (**c**) $y = -0.02x^2 + 0.09x + 1.86$, (**d**) $y = 0.02\sqrt{x} + 0.02$.

bioerosion rates in the Hawaiian Archipelago have found the highest bioerosion rates at Kahekili, Maui, a site with a significant influx of nutrient-rich SGD (Prouty et al. 2017; Silbiger et al. 2017), indicating that the relationship between SGD and bioerosion in the current study is not a localized phenomenon.

Nutrients can increase bioerosion rates by providing an ample food source for boring organisms, many of which are filter feeders (Glynn 1997). This relationship has been documented across eutrophication gradients on reefs around the world, including in Australia (e.g., Le Grand and Fabricius 2011), Indonesia (Edinger et al. 2000), and Barbados (Holmes

2000; also see Fabricius 2005 and Le Grand and Fabricius 2011 for reviews on this topic). Higher rates of microbioerosion were found in areas of mid- and high levels of nutrient-rich SGD on Reunion Island (Chazottes et al. 2002). This trend holds true on larger scales as well, with bioerosion increasing along a nutrient and pH gradient spanning the entire Pacific basin (DeCarlo et al. 2015). Nutrients and terrestrial inputs can also drive community composition to include more bioeroding organisms that benefit from nutrient input. For example, inshore reefs in Australia affected by freshwater runoff and sedimentation had higher levels of internal bioeroders, including boring sponges and polychaetes (Osorno et al. 2005).

pH effects on coral growth and bioerosion

Interestingly, mean pH had no significant effect on any of the response variables measured in this study, but pH variation had a significant negative effect on the percent change in buoyant weight and surface area of the corals. pH varied widely at both sites, with maximum ranges between 7.86 and 8.33 at Black Point and 7.85 and 8.20 at Wailupe, while the range in mean pH values was much smaller (7.99–8.08 across both sites). This variability is comparable to data recorded in other coastal systems (Hofmann et al. 2011; Price et al. 2012; Shaw et al. 2012; Duarte et al. 2013; Guadayol et al. 2014; Yates et al. 2007), and highlights the importance of including pH variability, rather than just mean pH, when examining the effects of ocean acidification on coastal organisms.

Price et al. (2012) identified duration and magnitude of daily pH maxima as predictors of calcification on reefs in the central Pacific, noting that more time spent at higher pH lead to higher rates of calcification. Likewise, corals in variable mangrove habitats where there was no buffering effect against low pH (as opposed to seagrass habitats, which saw high variability but overall higher pH) have been shown to have lower calcification rates (Camp et al. 2016). This is likely the case in Maunalua Bay as well; although mean pH did not vary greatly across space, experimental locations that experienced higher pH variation spent more time at low pH, leading to decreased calcification in the more variable locations. As water chemistry was driven primarily by SGD at these sites, it is possible that these reef communities do not have the capacity to buffer against SGD-driven changes in pH, thus maintaining low calcification rates.

These findings are consistent with studies of corals near groundwater seeps in Maui and Mexico, which found decreased calcification in corals exposed to SGD (Crook et al. 2013; Prouty et al. 2017). Both sites have been shown to have highly variable (e.g., range = 0.905 pH units over a 30 d period in Mexico; Hofmann et al. 2011), though generally low pH due to the discharge of SGD. However, when interpreted in the context of nutrient-enriched groundwater, the relationship is more complex, as coral nubbins collected from sites impacted by SGD were found to have higher calcification rates per unit surface area across Ω_{arag} treatments than those collected from non-SGD sites (Chauvin et al. 2011). This indicates that although changes in carbonate chemistry may lead to decreases in calcification, these effects may be mediated by the positive effects of SGD-derived nutrients. This relationship is consistent with other studies that have found a positive effect of nutrients on calcification rates in high pCO_2 conditions (Atkinson et al. 1995; Holcomb et al. 2010).

Interestingly, neither mean pH nor pH variation had a significant effect on bioerosion rates. Numerous studies have found increases in bioerosion rates under low pH conditions (e.g., Tribollet et al. 2009; Wisshak et al. 2012; Crook et al. 2013; Reyes-Nivia et al. 2013; Silbiger et al. 2014, 2016; Barkley et al. 2015; DeCarlo et al. 2015; Silbiger and Donahue 2015). However, most of these studies have seen a response due to differences in mean pH or across a range of fixed pCO_2 treatments, and have not explicitly tested the effect of pH variability. It is possible that the range in mean pH at our sites was not wide enough to detect a response in bioerosion rate and that the much wider range in nutrients overwhelmed the pH response. pH_{Tot} ranged from 7.85 to 8.33 in this study, whereas $NO_3^- + NO_2^-$, for example, ranged from 0.02 μmol L^{-1} to 32.39 μmol L^{-1}. Nutrients have been found to exacerbate the effect of acidification on bioerosion by tenfold (DeCarlo et al. 2015), suggesting that perhaps across our narrow gradient in mean pH, the effect of nutrients may be more pronounced.

Offshore sites

Although the offshore sites were not included in the formal analysis, for all coral growth metrics, mean values from these sites agreed well with data from the low %SGD experimental locations (Fig. 4). However, bioerosion was much higher than expected by the model at both outer sites, particularly Wailupe. This is likely due to higher rates of grazing by parrotfish and urchins on the forereef. Chazottes et al. (2002) found higher grazing rates and, therefore, higher overall bioerosion rates, by urchins on reefs without SGD input than on those with high or mid-levels of SGD. Parrotfish biomass at outer sites in Maunalua, although low (parrotfish biomass= 0.2 ± 0.2 g m^{-2} at Black Point, 1.3 ± 0.5 g m^{-2} at Wailupe), is comparable to other open or unprotected sites on O'ahu (Williams et al. 2009), and higher than the inshore sites included in this study, where no adult parrotfish were observed throughout the experiment (K. Lubarsky unpubl.). Indeed, the bioerosion rates at the outer sites are comparable to bioerosion rates found on reefs throughout the Hawaiian archipelago (Silbiger et al. 2017).

Accretion vs. bioerosion rates

Coral accretion rates were two orders of magnitude higher than bioerosion rates across both sites. Based only on rates, this indicates that nearshore reefs in Maunalua should be in a state of net accretion; however, this conclusion is

misleading for several reasons. Units of coral accretion are in kg m^{-2} of *live coral* per year, while bioerosion rates are in kg m^{-2} of *substrate* per year. Urbanization and land use change have led to marked decreases in coral cover in Maunalua Bay over the past century, and coral cover remains very low (Supporting Information Fig. 1), especially on the reef flats (Wolanski et al. 2009). Therefore, there is much more substrate available to bioeroders than is occupied by coral at these sites, and the total amount of $CaCO_3$ removed by bioeroders is almost certainly higher than the amount accreted by corals. In addition, our bioerosion blocks were only deployed for 1 yr and, therefore, only captured the early successional stages of the bioeroder community (Hutchings 1986; Silbiger et al. 2014). Bioerosion rates in similar experimental blocks were found to increase significantly between 2- and 4-yr deployments on the Great Barrier Reef (Osorno et al. 2005), indicating that measured bioerosion rates at our sites would likely be higher given a longer deployment time.

Water chemistry was only measured over two 24-h cycles at strong spring tides in this study in order to provide snapshots of the highest SGD-driven variability at these sites. Due to the experimental design, logistics prevented more frequent water sampling. However, the results of this study are comparable to other studies near SGD-seeps with higher resolution water chemistry data. For example, Prouty et al. (2017) measured similar water chemistry parameters across an SGD gradient in Maui every 4 h for 6 d, and found higher bioerosion rates and lower calcification rates near the SGD seep, and attributed these patterns to changes in pH, nutrients, and salinity of the SGD. Accretion and erosion in this study were measured from *P. lobata* cores across the gradient, indicating that these patterns are consistent over both the short time periods measured in our study, and when averaged over many years. Therefore, it is likely that the present sampling regime had sufficient resolution to identify drivers of coral growth and bioerosion at these sites.

Conclusions

The results of this study indicate that SGD is an important source of new nutrients to nearshore reef flats in Maunalua Bay. SGD-derived nutrients increase rates of coral growth and bioerosion, although at the highest SGD locations salinity stress induces mortality and decreases coral growth. The tidally modulated discharge of SGD to these sites delivers semi-diurnal pulses of low-sediment, nutrient-rich water onto the reef flat, which contrasts with the periodic inundations of nutrients and sediment by surface waters driven by precipitation. Whereas corals on reefs impacted by surface water may be nutrient-limited between pulses, the daily, moderate enrichment by SGD may relieve corals and bioeroders of nutrient limitation, allowing for higher growth and bioerosion rates.

In this study, calcification rates far exceeded rates of bioerosion. However, the extremely low coral cover in Maunalua Bay compared with dead substrate suggests that coral calcification likely does not exceed bioerosion at these sites. These findings suggest that urbanization and other land-use changes outlined in Wolanski et al. (2009), rather than SGD, are the cause for this reef degradation and subsequent dominance of erosional processes. They do, however, indicate that if corals are able to settle on these reef flats, they may sustain relatively high rates of growth near SGD seeps. Recent restoration efforts by community groups in the area have aimed at removing invasive algae from similar reef flats in the bay; although these efforts have not been implemented at our study sites, the results from this study indicate that in the absence of algal competition, corals can thrive on SGD-impacted reef flats, and suggest that management of these and similar local stressors such as sedimentation could aid in the recovery of coral populations on Maunalua Bay reef flats.

References

Andersson, A. J., and D. Gledhill. 2013. Ocean acidification and coral reefs: effects on breakdown, dissolution, and net ecosystem calcification. Annual Review of Marine Science **5**: 321–348. doi:10.1146/annurev-marine-121211-172241

Atkinson, M. J., B. Carlson, and G. L. Crow. 1995. Coral growth in high-nutrient, low-pH seawater: A case study of corals cultured at the Waikiki Aquarium, Honolulu, Hawai'i. Coral Reefs **14**: 215–223. doi:10.1007/BF00334344

Barkley, H. C., A. L. Cohen, Y. Golbuu, V. R. Starczack, T. M. DeCarlo, and K. E. F. Shamberger. 2015. Changes in coral reef communities across a natural gradient in seawater pH. Sci. Adv. **1**: e1500328. doi:10.1126/sciadv.1500328

Bongiorni, L., S. Shafir, D. Angel, and B. Rinkevich. 2003. Survival, growth and gonad development of two hermatypic corals subjected to in situ fish-farm nutrient enrichment. Mar. Ecol. Prog. Ser. **253**: 137–144. doi:10.3354/meps253137

Camp, E. F., D. J. Suggett, G. Gendron, J. Jompa, D. Manfrino, and D. J. Smith. 2016. Mangrove and seagrass beds provide different biogeochemical services for corals threatened by climate change. Front. Mar. Sci. **3**: 52. doi:10.3389/fmars.2016.00052

Chauvin, A., V. Denis, and P. Cuet. 2011. Is the response of coral calcification to seawater acidification related to nutrient loading? Coral Reefs **30**: 911–923. doi:10.1007/s00338-011-0786-7

Chazottes, V., T. L. Campion-Alsumard, M. Peyrot-Clausade, and P. Cuet. 2002. The effects of eutrophication-related alterations to coral reef communities on agents and rates of bioerosion (Reunion Island, Indian Ocean). Coral Reefs **21**: 375–390. doi:10.1007/s00338-002-0259-0

Crook, E. D., A. L. Cohen, M. Robolledo-Vieyera, L. Hernandez, and A. Paytan. 2013. Reduced calcification

and lack of acclimatization by coral colonies growing in areas of persistent natural acidification. Proc. Natl. Acad. Sci. USA **110**: 11044–11049. doi:10.1073/pnas.1301589110

Cyronak, T., I. R. Santos, D. V. Erler, and B. D. Eyre. 2013. Groundwater and porewater as major sources of alkalinity to a fringing coral reef lagoon (Muri Lagoon, Cook Islands). Biogeosciences **10**: 2467–2480. doi:10.5194/bg-10-2467-2013

Cyronak, T., I. R. Santos, D. V. Erler, D. T. Maher, and B. D. Eyre. 2014. Drivers of pCO_2 variability in two contrasting coral reef lagoons: The influence of submarine groundwater discharge. Global Biogeochem. Cycles **28**: 398–414. doi:10.1002/2013GB004598

DeCarlo, T. M., A. L. Cohen, H. C. Barkley, Q. Cobban, C. Young, K. E. Shamberger, R. E. Brainard, and Y. Golbuu. 2015. Coral macrobioerosion is accelerated by ocean acidification and nutrients. Geology **43**: 7–10. doi:10.1130/G36147.1

Dickson, A. G., C. L. Sabine, and J. R. Christian. 2007. Guide to best practices for ocean CO_2 measurements, p. 176. PICES special publication 3. North Pacific Marine Science Organization.

Dimova, N. T., P. W. Swarzenski, H. Dulaiova, and C. R. Glenn. 2012. Utilizing multichannel electrical resistivity methods to examine the dynamics of the fresh water-seawater interface in two Hawaiian groundwater systems. J. Geophys. Res. Oceans **117**: C02012. doi:10.1029/2011JC007509

Doty, M. S. 1971. Measurement of water movement in reference to benthic algal growth. Bot. Mar. **14**: 32–35. doi:10.1515/botm.1971.14.1.32

Drupp, P., E. H. De Carlo, F. T. Mackenzie, P. Bienfang, and C. L. Sabine. 2011. Nutrient inputs, phytoplankton response, and CO_2 variations in a semi-enclosed subtropical embayment, Kāne'ohe Bay, Hawai'i. Aquat. Geochem. **17**: 473–498. doi:10.1007/s10498-010-9115-y

Duarte, C. M., and others. 2013. Is ocean acidification an open-ocean syndrome? Understanding anthropogenic impacts on seawater pH. Estuaries Coast. **36**: 221–236. doi:10.1007/s12237-013-9594-3

Edinger, E. N., G. V. Limmon, J. Jompa, W. Widjatmoko, J. M. Heikoop, and M. J. Risk. 2000. Normal coral growth rates on dying reefs: Are coral growth rates good indicators of reef health? Mar. Pollut. Bull. **40**: 404–425. doi:10.1016/S0025-326X(99)00237-4

Fabricius, K. E. 2005. Effects of terrestrial runoff on the ecology of corals and coral reefs: Review and synthesis. Mar. Pollut. Bull. **50**: 125–146. doi:10.1016/j.marpolbul.2004.11.028

Forsman, Z. H., B. Rinkevich, and C. L. Hunter. 2006. Investigating fragment size for culturing reef-building corals (*Porites lobata* and *P. compressa*) in *ex situ* nurseries. Aquaculture **261**: 89–97. doi:10.1016/j.aquaculture.2006.06.040

Franklin, E. C., M. J. Donahue, and P. L. Jokiel. 2013. Predictive modeling of coral distribution and abundance in the Hawaiian Islands. Mar. Ecol. Prog. Ser. **481**: 121–132. doi:10.3354/meps10252

Glynn, P. W. 1997. Bioerosion and coral reef growth: A dynamic balance, p. 69–98. *In* C. Birkeland [ed.], Life and death of coral reefs. Chapman and Hall.

Grottoli, A. G. 1999. Variability of stable isotopes and maximum linear extension in reef-coral skeletons at Kāne'ohe Bay, Hawai'i. Mar. Biol. **135**: 437–449. doi:10.1007/s002270050644

Guadayol, Ò., N. J. Silbiger, M. J. Donahue, and F. I. M. Thomas. 2014. Patterns in temporal variability of temperature, oxygen and pH along an environmental gradient in a coral reef. PLoS One **9**: e85213. doi:10.1371/journal.pone.0085213

Hofmann, G. E., and others. 2011. High-frequency dynamics of ocean pH: A multi-ecosystem comparison. PLoS One **6**: e28983. doi:10.1371/journal.pone.0028983

Holcomb, M., D. C. McCorkle, and A. L. Cohen. 2010. Long-term effects of nutrient and CO_2 enrichment on the temperate coral *Astrangia poculata* (Ellis and Solander, 1786). J. Exp. Mar. Biol. Ecol. **386**: 27–33. doi:10.1016/j.jembe.2010.02.007

Holmes, K. E. 2000. Effects of eutrophication on bioeroding sponge communities with the description of new West Indian sponges, *Cliona spp*. (Porifera : Hadromerida : Clionidae). Invertebr. Biol. **119**: 125–138. doi:10.1111/j.1744-7410.2000.tb00001.x

Hutchings, P. A. 1986. Biological destruction of coral reefs: A review. Coral Reefs **4**: 239–252. doi:10.1007/BF00298083

Johnson, A. G., C. R. Glenn, W. C. Burnett, R. N. Peterson, and P. G. Lucey. 2008. Aerial infrared imaging reveals large nutrient-rich groundwater inputs to the ocean. Geophys. Res. Lett. **35**: L15606. doi:10.1029/2008GL034574

Jokiel, P. J., J. E. Maragos, and L. Franzisket. 1978. Coral growth: Buoyant weight technique, p. 529–541. *In* D. R. Stoddart and R. E. Johannes [eds.], Coral reefs: Research methods. UNESCO.

Jokiel, P. L., and J. L. Morrissey. 1993. Water motion on coral reefs: Evaluation of the "clod card" technique. Mar. Ecol. Prog. Ser. **93**: 175–181. doi:10.3354/meps093175

Le Grand, H. M., and K. E. Fabricius. 2011. Relationship of internal macrobioeroder densities in living massive Porites to turbidity and chlorophyll on the Australian Great Barrier Reef. Coral Reefs **30**: 97–107. doi:10.1007/s00338-010-0670-x

Lee, J., and G. Kim. 2015. Dependence of coastal water pH increases on submarine groundwater discharge off a volcanic island. Estuar. Coast. Shelf Sci. **163**: 15–21. doi:10.1016/j.ecss.2015.05.037

Lewis, E., and D. Wallace. 1998. Program developed for CO_2 system calculations. ORNL/CDIAC-105. Carbon Dioxide Information Analysis Center, Oak Ridge National Laboratory, US Department of Energy.

Moosdorf, N., T. Stieglitz, H. Waska, H. H. Dürr, and J. Hartmann. 2015. Submarine groundwater discharge from

tropical islands: A review. Grundwasser **20**: 53–67. doi:10.1007/s00767-014-0275-3

Nairn, O. 1993. Seasonal responses of a fringing reef community to eutrophication (Reunion Island, Western Indian Ocean). Mar. Ecol. Prog. Ser. **99**: 137–151. doi:10.3354/meps099137

Nelson, C. E., and others. 2015. Fluorescent dissolved organic matter as a multivariate biogeochemical tracer of submarine groundwater discharge in coral reef ecosystems. Mar. Chem. **177**: 232–243. doi:10.1016/j.marchem.2015.06.026

Osorno, A., M. Peyrot-Clausade, and P. A. Hutchings. 2005. Patterns and rates of erosion in dead Porites across the Great Barrier Reef (Australia) after 2 years and 4 years of exposure. Coral Reefs **24**: 292–303. doi:10.1007/s00338-005-0478-2

Pandolfi, J. M., S. R. Connolly, D. J. Marshall, and A. L. Cohen. 2011. Projecting coral reef futures under global warming and ocean acidification. Science **333**: 418–422. doi:10.1126/science.1204794

Paytan, A., G. G. Shellenbarger, J. H. Street, M. E. Gonneea, K. Davis, M. B. Young, and W. S. Moore. 2006. Submarine groundwater discharge: An important source of new inorganic nitrogen to coral reef ecosystems. Limnol. Oceanogr. **51**: 343–348. doi:10.4319/lo.2006.51.1.0343

Price, N. N., T. R. Martz, R. E. Brainard, and J. E. Smith. 2012. Diel variability in seawater pH relates to calcification and benthic community structure on coral reefs. PLoS One **7**: e43843. doi:10.1371/journal.pone.0043843

Prouty, N. G., A. Cohen, K. K. Yates, C. D. Storlazzi, P. W. Swarzenski, and D. White. 2017. Vulnerability of coral reefs to bioerosion from land-based sources of pollution. J. Geophys. Res. Oceans **122**: 9319–9331. doi:10.1002/2017JC013264

Prouty, N. G., K. K. Yates, N. Smiley, C. Gallagher, O. Cheriton, and C. D. Storlazzi. 2018. Carbonate System Parameters of an Algal-dominated Reef along West Maui, Biogeosciences Discuss., in review. doi:10.5194/bg-2018-35

Reyes-Nivia, C., G. Diaz-Pulido, D. Kline, O. Hoegh-Guldberg, and S. Dove. 2013. Ocean acidification and warming scenarios increase microbioerosion of coral skeletons. Glob. Chang. Biol. **19**: 1919–1929. doi:10.1111/gcb.12158

Richardson, C. M., H. Dulai, and R. B. Whittier. 2017a. Sources and spatial variability of groundwater-delivered nutrients in Maunalua Bay, O'ahu, Hawai'i. J. Hydrol. Reg. Stud. **11**: 178–193. doi:10.1016/j.ejrh.2015.11.006

Richardson, C. M., H. Dulai, B. N. Popp, K. Ruttenberg, and J. K. Fackrell. 2017b. Submarine groundwater discharge drives biogeochemistry in two Hawaiian Reefs. Limnol. Oceanogr. **62**: S348–S363. doi:10.1002/lno.10654

Sawall, Y., M. C. Teichberg, J. Seemann, M. Litaay, J. Jompa, and C. Richter. 2011. Nutritional status and metabolism of the coral *Stylophora subseriata* along a eutrophication gradient in Spermonde Archipelago (Indonesia). Coral Reefs **30**: 841–853. doi:10.1007/s00338-011-0764-0

Shaw, E. C., B. I. McNeil, and B. Tilbrook. 2012. Impacts of ocean acidification in naturally variable coral reef flat ecosystems. J. Geophys. Res. Oceans **117**: C03038. doi:10.1029/2011JC007655

Silbiger, N. J., O. Guadayol, F. I. M. Thomas, and M. J. Donahue. 2014. Reefs shift from net accretion to net erosion along a natural environmental gradient. Mar. Ecol. Prog. Ser. **515**: 33–44. doi:10.3354/meps10999

Silbiger, N. J., and M. J. Donahue. 2015. Secondary calcification and dissolution respond differently to future ocean conditions. Biogeosciences **12**: 567–578. doi:10.5194/bg-12-567-2015

Silbiger, N. J., O. Guadayol, F. I. M. Thomas, and M. J. Donahue. 2016. A novel μCT analysis reveals different responses of bioerosion and secondary accretion to environmental variability. PLoS One **11**: e0153058. doi:10.1371/journal.pone.0153058

Silbiger, N. J., M. J. Donahue, and R. E. Brainard. 2017. Environmental drivers of coral reef carbonate production and bioerosion: A multi-scale analysis. Ecology **98**: 2547–2560. doi:10.1002/ecy.1946

Street, J. H., K. L. Knee, E. E. Grossman, and A. Paytan. 2008. Submarine groundwater discharge and nutrient addition to the coastal zone and coral reefs of leeward Hawai'i. Mar. Chem. **109**: 355–376. doi:10.1016/j.marchem.2007.08.009

Swarzenski, P. W., H. Dulaiova, M. L. Dailer, C. R. Glenn, C. G. Smith, and C. D. Storlazzi. 2013. A geochemical and geophysical assesment of coastal groundwater discharge at select sites in Maui and O'ahu, Hawai'i, p. 27–46. *In* C. Wetzelhuetter [ed.], Groundwater in the coastal zones of Asia-Pacific. Springer.

Tanaka, Y., T. Miyajima, I. Koike, T. Hayashibara, and H. Ogawa. 2007. Imbalanced coral growth between organic tissue and carbonate skeleton caused by nutrient enrichment. Limnol. Oceanogr. **52**: 1139–1146. doi:10.4319/lo.2007.52.3.1139

Tribollet, A., C. Godinot, M. Atkinson, and C. Langdon. 2009. Effects of elevated pCO_2 on dissolution of coral carbonates by microbial euendoliths. Global Biogeochem. Cycles **23**: GB3008. doi:10.1029/2008GB003286

Wang, G., W. Jing, S. Wang, Y. Xu, Z. Wang, Z. Zhang, Q. Li, and M. Dai. 2014. Coastal acidification induced by tidal-driven submarine groundwater discharge in a coastal coral reef system. Environ. Sci. Technol. **48**: 13069–13075. doi:10.1021/es5026867

Williams, I. D., M. Mejia, Z. R. Caldwell, K. S. Pollock, and E. J. Conklin. 2009. Nature conservancy of Hawaii Maunalua marine survey report. The Nature Conservancy.

Wisshak, M., C. H. L. Schönberg, A. Form, and A. Freiwald. 2012. Ocean acidification accelerates reef bioerosion. PLoS One **7**: e45124. doi:10.1371/journal.pone.0045124

Wolanski, E., J. A. Martinez, and R. H. Richmond. 2009. Quantifying the impact of watershed urbanization on a coral reef: Maunalua Bay, Hawai'i. Estuar. Coast. Shelf Sci. **84**: 259–268. doi:10.1016/j.ecss.2009.06.029

Yates, K. K., C. Dufore, N. Smiley, C. Jackson, and R. B. Halley. 2007. Diurnal variation of oxygen and carbonate system parameters in Tampa Bay and Florida Bay. Mar. Chem. **104**: 110–124. doi:10.1016/j.marchem.2006.12.008

Acknowledgments

We would like to thank our collaborators F. Thomas, H. Dulaiova, C. Nelson, F. LaValle, C. Richardson, S. Goldberg, and E. Franklin for their advice and support throughout the study. Field and lab help was provided by several volunteers; in particular, we would like to thank J. Kuwabara, A. Kirby, E. Nalley, J. Zill, C. Counsell, J. Caldwell, I. Caldwell, C. Couch, H. Shiu, E. Lenz, J. Davidson, H. Putnam, B. Day, N. Jones, and Z. Forsman. This project was supported by the NSF Graduate Research Fellowship Program (DGE-1329626) to KAL, the NOAA Nancy Foster Scholarship Program to NJS, and the University of Hawai'i SeaGrant Program (NA14OAR4170071-R/SB-10) to MJD. This paper is funded by a grant from the National Oceanic and Atmospheric Administration, Project R/SB-10, which is sponsored by the University of Hawaii Sea Grant College Program, SOEST, under Institutional Grant NA14OAR4170071 from NOAA Office of Sea Grant, Department of Commerce. The views expressed herein are those of the authors and do not necessarily reflect the views of NOAA or any of its subagencies. UNIHI-SEAGRANT-JC-14-47. This is contribution number 265 from the CSUN Marine Biology Program, number 1720 from the Hawai'i Institute of Marine Biology, and number 10325 from SOEST.

Conflict of Interest

None declared.

Submitted 03 July 2017
Revised 30 November 2017
Accepted 06 February 2018

Associate editor: Bradley Eyre